

# Performance Analysis of Focus Measures in a SFF-Inspired Approach for Sparse Scene Reconstruction

<sup>1</sup>R. Senthilnathan\*, <sup>2</sup>P. Subhasree, <sup>2</sup>R. Sivaramakrishnan, <sup>3</sup>C. R. Srinivasan and <sup>3</sup>R. Srividya

**Abstract:** Shape From Focus (SFF) is a popular technique in the field of computer vision for scene reconstruction. The SFF technique is based on the fact that the focus levels of the pixels of the image preserves depth information. The usage of telecentric lenses for conventional SFF limits its application for only small objects so as to preserve magnification constancy. In the current research work a new SFF-inspired algorithm is developed which utilizes a wide angle lens in place of a telecentric lens. This extends the range of object that the system can deal with, though severe magnification changes occur when a stack of images are acquired with respect to the scene. This problem is addressed using a variable window approach when focus measures are computed. This paper is a segment of the larger research work which aims at evaluation of 15 different focus measures. The paper presents significant results of performance evaluation of four different focus measures most commonly used in SFF and auto-focus algorithms. The evaluation is carried out based on two different performance evaluation criteria namely root mean square error and computation time. The analysis of focus measures are carried out under various operating conditions such as different spatial resolution, window size, contrast changes, gray level saturation and camera noise.

**Keywords:** Shape from Focus, Variable Magnification, Variable Window Size, Focus Measures

## 1. INTRODUCTION

Computer vision is one of the most researched field and has many application in many fields like computer aided inspection, robotics, entertainment and other scientific and industrial applications. Scene reconstruction is the most important problem addressed in the field of 3-D Computer Vision. Out of these methods available for scene reconstruction Shape from Focus (SFF) [1] and Shape from Defocus (SFD) use multiple images of the scene taken with varying focus levels. The difference between the methods come the in the form that the SFD [2] generally require one sharp image of the foreground and one sharp image of the background. The distance of all the points that lie between background and foreground is interpolated by a sharpness measure. Unlike the SFD method, SFF generally requires more number of images acquired along different focal distances. This generally makes the SFF method time consuming and computationally tedious compared to SFD, though the precision of reconstruction in SFF is better than SFD. The SFF techniques have been successfully used in medical diagnostics, computer aided inspection involving microscopic imaging or imaging of small objects [3]. The SFF techniques demand images of the scene to be acquired from different focal distances which can be obtained by translating the camera or the object or by changing the focus setting of the lens. One of the basic limitations of the SFF method is that it is highly sensitive to magnifications changes. Many authors in the recent in years have presented

<sup>1</sup> Department of Mechatronics Engineering, SRM University, Kattankulathur

<sup>2</sup> Division of Mechatronics, Department of Production Technology, MIT Campus, Anna University

<sup>3</sup> Manipal Institute of Technology, Manipal University  
e-mail: senthilmnathan.r@ktr.srmuniv.ac.in

methods to improve the applicability of SFF techniques by means of novel image processing procedures [4]. The attempts made for increasing the applicability of the SFF technique is purely for complete scene reconstruction rather than using some approximate information from SFF with an imaging system prone to magnification changes across the focal stack. This paper reports a small part of the research work which deals with development of an algorithm inspired by conventional SFF which may be used for scenario involving parallax. Previous work from the authors presented results of evaluation of focus measures based on image gradient. This paper presents results of evaluation of four other focus measures commonly used in autofocus and SFF procedures. Since the current paper is only part of a larger research work most of the common introductory contents are carried over from the previous articles [5, 6].

## 2. PROPOSED SFF-INSPIRED ALGORITHM

As mentioned in the previous section of the paper the setup required for SFF demands a precise translating mechanism. The photograph of the experimental setup is shown in Fig. 1. The images are taken on the go using time-synchronization approach and hence a simple DC motor is used for the purpose.

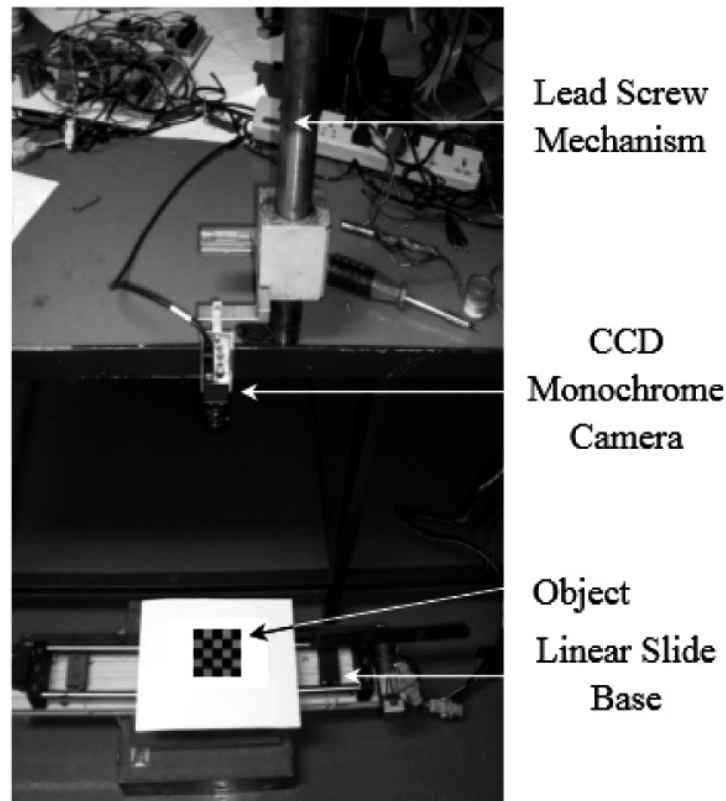


Figure 1: Experimental Setup

The various specifications of the imaging system are shown in Table 1. A focus measure is basically a mathematical function, which gives a measure of the focus of the image indirectly, by measuring the contrast of the image. It is generally computed in a small square window around the pixels in the image. A high value for the focus measure indicates a sharply focussed region in the image, and a low value indicates blurred regions. Most focus measures presented in SFF and autofocus algorithms are based on either image derivative or statistical information of the image content. The following section presents four important methods used in the current study that do not fall under any of the previously mentioned three categories.

**Table 1**  
**System Specifications**

<i>Parameter</i>	<i>Specification</i>	<i>Parameter</i>	<i>Specification</i>
Light Source	White LED area light	Aspect Ratio	4:3
Illuminance	160 lux	Sensor	Sony ICX424
Lighting Technique	Partially diffused bright field incident lighting	Sensor Type	CCD Progressive, Monochrome
Lens Type	Fixed focal length prime lens	Operating Frame Rate	45 Frames Per Second
Focal Length & f#	16 mm and 1.3	Mode of operation	Mono8 mode
Camera Make and Model	Allied Vision Technologies Guppy F033b	Trigger Type	Software trigger
Interface	IEEE 1394a – 400Mb/s, 1 port	Image Acquisition Time	180ms per image
Computer Interface	PCI – IEEE 1394a	Processor	Intel Core i5, 2.5GHz
Resolution	640 × 480	Memory	4 GB, 1300 MHz

A focus measure based on the second difference of the grey levels of the image in the neighborhood  $\Omega$  is termed as Brenner's measure [7]. The focus measure is given by,

$$F_B = \sum_{(i,j) \in \Omega(x,y)} |I(i,j) - I(i+2j)|^2 \quad (1)$$

Usage of the image contrast as a focus measure for autofocus was reported in [8]. The image contrast may be defined

$$F_{IC} = \sum_{(i,j) \in \Omega(x,y)} C(i,j) \quad (2)$$

Where  $C(i,j)$  is the accumulated image contrast in the local neighbourhood  $\Omega$  given by,

$$C(x,y) = \sum_{i=x-1}^{x+1} \sum_{j=y-1}^{y+1} |I(x,y) - I(i,j)| \quad (3)$$

An operator, named as image curvature, applied to microscopy was reported in [9]. If the relation between the discrete grey levels is interpolated by means of a surface, the curvature may be used as a focus measure [10]. The curvature may be computed as

$$F_{ICU} = |c_0| + |c_1| + |c_2| + |c_3| \quad (4)$$

Where  $C = (c_0, c_1, c_2, c_3)^T$  is the vector of coefficients used to interpolate the quadratic surface  $f(x,y) = c_0x + c_1y + c_2x^2 + c_3y^2$ .  $C$  is computed through least squares by applying two convolution masks as follows:

$$c_0 = M_1 * I, c_1 = M_1^T * I, c_2 = \frac{3}{2} M_2 * I - M_2^T * I \text{ and } c_3 = \frac{3}{2} M_2^T * I - M_2 * I \quad (5)$$

where

$$M_1 = \frac{1}{6} \begin{pmatrix} -1 & 0 & 1 \\ -1 & 0 & 1 \\ -1 & 0 & 1 \end{pmatrix} \text{ and } M_2 = \frac{1}{5} \begin{pmatrix} 1 & 0 & 1 \\ 1 & 0 & 1 \\ 1 & 0 & 1 \end{pmatrix} \quad (6)$$

A focus measure based on the image autocorrelation is presented in [11] for autofocus, which may be adopted for measuring the focus in SFF. The function is called as Vollath's autocorrelation, and is defined as follows:

$$F_{VC} = \sum_{(i,j) \in \Omega(x,y)} (I(i,j) \cdot I(i+1,j)) - \sum_{(i,j) \in \Omega(x,y)} (I(i,j) \cdot I(i+2,j)) \quad (7)$$

The following section of the paper presents the proposed SFF-inspired algorithm, which forms the central theme of the larger research work, a portion of which is presented in this paper. First a set of feature points present across the stack of images is detected using Speeded-Up Robust Features (SURF) feature detector [12]. The stack suffers from combined variations in focus and magnification because of the relative motion between the camera and the scene. The focus measure of only those particular pixels is computed. This is different from the conventional SFF route, where the focus measure is computed for all the pixels in all the images in the focal stack. In the current research, since a wide angle lens is used with a higher DOF, in order to achieve a complete Gaussian distribution, large camera motion would be required. Extremely low magnification causes the spatial resolution of the image to become too poor for any measurements possible from the images. Because of these reasons a coarse method of depth estimate is adopted for this research. The algorithm may be summarized as follows:

- i. The initial location of the camera from the measurement plane is known a priori as  $s_m$ , where  $m = 1$  for the initial location of the camera.
- ii. Accumulate the image sequences acquired at each step  $m$  where the stand-off distance ( $s_m$ ) increases in steps of  $\Delta d$ .
- iii. Measure focus,  $F_m$  for each of the SURF feature points, across the stack at each step whose correspondences are matched using the SSD metric.
- iv. Find the step number  $m$  in which the focus measure is the maximum for a point  $(x, y)$ , such that  $F_m = F_{max}$ , where  $F_{max}$  is the maximum value of the focus measure for a particular pixel.
- v. Assign the value of the distance of the camera motion as the height of the object corresponding to the particular pixel, such that the height of the scene point  $\bar{h} = m\Delta d$ .
- vi. Once the height of a point is computed, the depth of the point  $C_z$  may be computed as  $C_z = s_l - \bar{h}$ .

This algorithm, as may be observed, gives only a rough estimate of the depth. The performance of the algorithm is directly dependent on the selection of  $\Delta d$ . Lower values of  $\Delta d$  give better accuracy, albeit there is always a non-zero resolution error. Interestingly, at times the estimated depth becomes equal to the actual depth, depending on the particular scene point under consideration. In other words the depth error may be zero, although the system as a whole suffers from a non-zero resolution error. The size of the window about which the focus measure is computed, is a vital parameter in the SFF method. Generally, the window size must be as small as possible to obtain accurate results. When the size of the window is large, a large neighbourhood is included to compute the focus. If the depth of the scene corresponding to different points in the window varies, it may lead to averaging of different focus levels caused by different depths of the scene points. In the current research, since the images suffer from magnification changes, a variable window size approach is developed. According to this method, the window size applied to a particular frame is scaled by the magnification factor corresponding to that frame. This means that in the current scenario, the window sizes would be reducing, starting from the first frame to the fifteenth image in the focal stack. Larger window sizes offer better results, but lead to averaging errors. It is justified, since the current work which uses the SFF-inspired algorithm only to obtain a sparse and coarse depth estimate. This issue may be considered as a drawback of the proposed method, as it inherently suffers from slightly higher averaging errors compared to the conventional SFF.

### 3. EVALUATION OF FOCUS MEASURES

The focus measures are evaluated under different operating conditions namely different spatial resolutions, camera noise, gray level saturation and contrast. Fig. 3 shows the stacks of three different spatial resolutions and the first image in each stack. The distances between the object and the measurement plane in the three cases are, 30 mm, 50 mm and 84 mm respectively. The three cases are indicated as spatial resolution 1, 2 and 3 respectively. Out of various camera noises that may corrupt an image acquired from a CCD sensor, the significant noise sources may be grouped as irradiance-dependent and irradiance-independent sources [13]. The noises may be modelled as follows:

$$I_{noise} = F(I + n_s + n_c) + n_q \quad (8)$$

where  $I_{noise}$  is the image that is obtained after adding the noise components to the original image  $I$ . The parameter  $F$  in the above equation is the camera response function,  $n_s$  is the irradiance-dependent noise component,  $n_c$  is the irradiance-independent noise component, and  $n_q$  is the quantization and amplification noise. The noise components are basically Gaussian white noise with zero mean, and the variances for  $n_s$  and  $n_c$  are  $Var(n_s) = I \cdot \sigma_s^2$  and  $Var(n_c) = \sigma_c^2$  respectively. The feature detectors and match metrics are evaluated for three different levels of noise, namely, for  $\sigma_s = \sigma_c = 0.0005$ ,  $\sigma_s = \sigma_c = 0.001$  and  $\sigma_s = \sigma_c = 0.002$ . Fig. 2 shows a magnified view of a small portion in the image (highlighted in red colour) which is subjected to different levels of noise corruption.

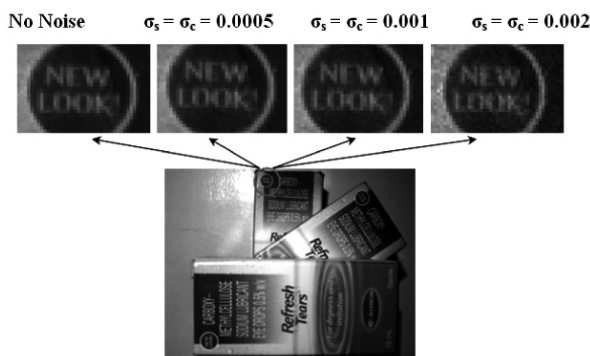


Figure 2: Different Noise levels

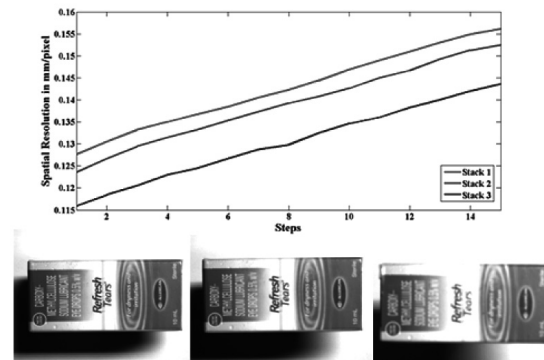


Figure 3: Different Spatial Resolution

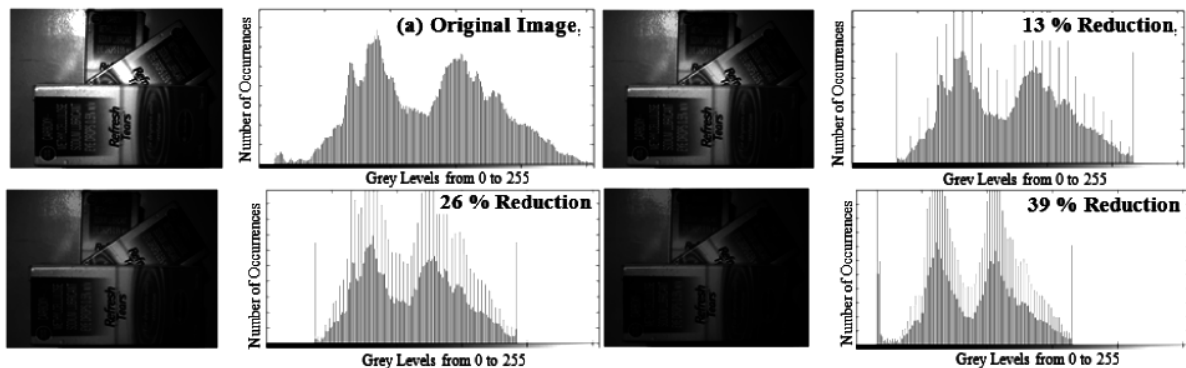


Figure 4: Contrast Reduction



Figure 5: Saturation Levels

Image contrast is an important factor that affects the performance of the algorithms, related to feature detection and matching. In the current study, the contrast of the original images is reduced to different levels to analyse the robustness of the detectors in such a scenario. The contrasts of the images are reduced by compressing the histogram of the respective images. Three different set of points are chosen, to achieve 13 %, 26 % and 39 % contrast reduction, with reference to the original images. Fig. 4 shows the first image of the focal stack for different contrast levels and their corresponding grey level histogram.

In this research, image saturation has been evaluated by adding a constant offset to the original image, as presented in the equation below:

$$I_{sat} = I + S \quad (9)$$

where  $I_{sat}$  is the saturated image obtained by adding a constant offset  $S$  to the original image  $I$ . In the current study, three different offsets, namely, 25, 51, 77 are added to the images, which may be considered as 10 %, 20 % and 30 % saturation respectively, for an 8-bit dynamic range. Fig. 5 shows the sample images subjected to various levels of saturation considered for evaluation. In the current research, two criteria are used for the evaluation of the focus measures under different operating conditions, namely, the execution time of the focus measures, and the Root Mean Square Error (RMSE). The RMSE is normalized by the number of pixels in the image and the number of steps of image acquisition. The normalized RMSE is defined as follows:

$$RMSE = \frac{\sqrt{\frac{1}{MN} \sum_{(i,j)} (G_T(i,j) - Z(i,j))^2}}{\text{No. of Steps}} \quad (10)$$

In the above equation  $N$  and  $M$  are the number of pixels in the horizontal and vertical dimensions of the image.  $G_T(i,j)$  is the ground truth information about the actual depth of a point  $(i,j)$  in the scene, and  $Z(i,j)$  is the estimated depth of the scene obtained from a particular focus measure at that point. The values of  $G_T(i,j)$  are found, based on the physical measurements of the object's dimensions, with an uncertainty of 1mm. The execution time is calculated by software means in MATLAB, which gives an approximate estimate of the time taken for the execution of a set of functions. In order to reduce error, the execution time is averaged from 20 trials for the same function's execution, and also all other application software is prevented from running.

The following plots in Fig. 6 show the results of RMSE for various operating conditions.

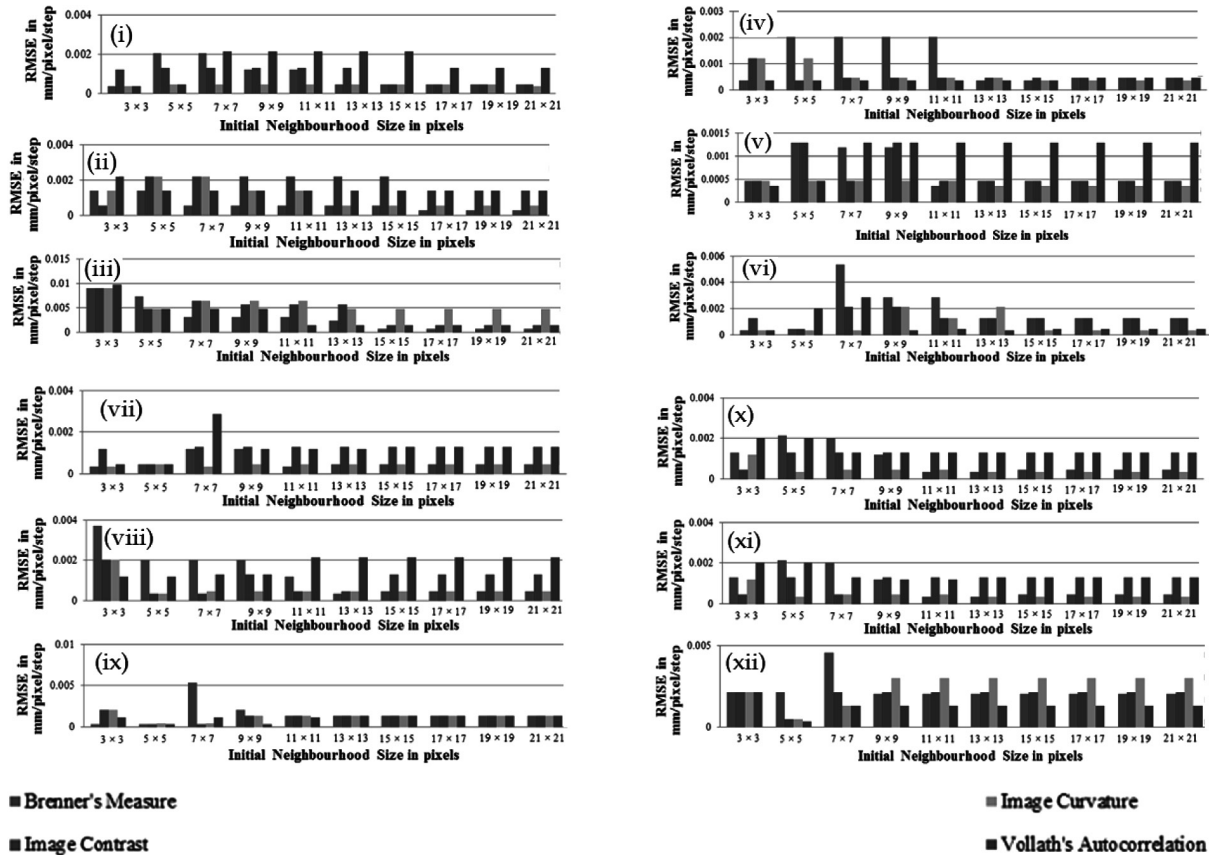


Figure 6: Results of RMSE for (i) Spatial Resolution 1 (ii) Spatial Resolution 2 (iii) Spatial Resolution 3 (iv) Camera Noise Level 1 (v) Camera Noise Level 2 (vi) Camera Noise Level 3 (vii) 13% Contrast Reduction (viii) 26% Contrast Reduction (ix) 39% Contrast Reduction (x) 10% Saturation (xi) 20% Saturation (xii) 30% Saturation

The average execution time for the four focus measures for a single point computed around a window are 0.175ms, 156.962ms, 3.641ms and 0.35ms respectively. The initial size of the window is  $21 \times 21$ , since the execution time for a larger window takes more time, compared to a smaller window; hence, evaluating in the worst case scenario. Based on the results it may be noted that the Brenner's measure and Image Curvature returned the least error. The Image Curvature takes the most time, mainly attributed by the iterative nature and the number of coefficients involved in the computation. Brenner's measure took the least and hence out of the four measures considered for evaluation Brenner's measure was found to be the effective algorithm. Higher window sizes returned lower RMSE. This is mainly due to the larger neighbourhood of focus measure which makes the measurement robust (at the cost of higher computational time) compared to the noise measurements obtained from smaller masks. Selection of a unique size is subjected to the trade off and a window size of  $15 \times 15$  is chosen to be the candidate window size for all the focus measurement purpose.

## References

- [1] S. K. Nayar, and Y. Nakagawa, "Shape from focus: An Effective Approach for Rough Surfaces," *CRA90*, pp. 218-225, 1990.
- [2] Y. Xiong and S. A. Shafer, "Depth from focusing and defocusing," *IEEE Computer Vision Pattern Recognition*, pp. 68-73, 1993.

- 
- [3] F. S. Helmlí and S. Scherer, "Adaptive shape from focus with an error estimation in light microscopy," *Proc. of 2nd International Symposium on Image and Signal Processing and Analysis*, 2001.
- [4] R. R. Sahay and A. N. Rajagopalan, "Dealing with Parallax In Shape-From-Focus," *IEEE Transactions on Image Processing*, Vol. 20 No. 2, pp. 558-569, 2011.
- [5] R. Senthilnathan and R. Sivaramakrishnan, "Estimation of relative depth in the scene using SFF-inspired focus cue," *Proc. of the IEEE International Conference on Advanced Communication Control and Computing Technologies ICACCCT*, pp. 332-337, 2012.
- [6] R. Senthilnathan, P. Subhasree and R. Sivaramakrishnan, "Performance Analysis of Gradient-Based Focus Measures in a Parallax Affected SFF Scenario," *International Journal of Computer Aided Manufacturing*, Vol. 1 No. 1, pp. 1-12, 2015.
- [7] Y. Sun, S. Duthaler and B. J. Nelson, "Autofocusing in computer microscopy: selecting the optimal focus algorithm," *Microscopy Research and Technique*, Vol. 65, pp. 139-149, 2004.
- [8] H. Nanda and R. Cutler, "Practical Calibrations for a Real-Time Digital Omni-directional Camera," *Proc. of International Conference on Computer Vision and Pattern Recognition*, pp. 1-8, 2001.
- [9] F. S. Helmlí and S. Scherer, "Adaptive shape from focus with error estimation in light microscopy," *Proc. of International Symposium on Image and Signal Processing and Analysis*, pp. 188-193, 2001.
- [10] R. Minhas, A. A. Mohammed, Q. M. Wu and M. A. Sid Ahmed, "3-D shape from focus and depth map computation using steerable filters," *Proc. of the International Conference on Image Analysis and Recognition*, pp. 573-583, 2009.
- [11] V. Hilsenstein, "Robust auto focusing for automated microscopy imaging of fluorescently labelled bacteria," *Proc. of the Digital Image Computing: Techniques and Applications*, 15, 2005.
- [12] H. Bay, T. Tuytelaars and L. Van Gool, "SURF: Speeded up robust features," *Proc. of European Conference on Computer Vision*, pp. 404-417, 2006.
- [13] S. Pertuz, D. Puig and M. A. Garcia, "Analysis of focus measure operators for shape-from-focus," *Pattern Recognition*, Vol. 46, pp. 1415-1432, 2013.